

Nano-structured vanadium: processing and mechanical properties under quasi-static and dynamic compression

Q. Wei ^{a,*}, T. Jiao ^a, K.T. Ramesh ^a, E. Ma ^b

^a Department of Mechanical Engineering, The Johns Hopkins University, 223 Latrobe Hall, Baltimore, MD 21218, USA

^b Department of Materials Science and Engineering, The Johns Hopkins University, Baltimore, MD 21218, USA

Received 29 July 2003; received in revised form 16 September 2003; accepted 9 October 2003

Abstract

We have processed fully dense, nano-structured vanadium (V), a bcc metal with a moderately high melting temperature (1910 °C) by high-energy ball milling followed by two-step consolidation. We have characterized the as-milled powder and the microstructure of the consolidated, fully dense material using X-ray diffraction and transmission electron microscopy. It was found that the grain size of the consolidated V is around 100 nm. Mechanical properties of the nano-structured V were studied under both quasi-static (strain rates in the range of 10^{-3} – 10^0 s⁻¹) and dynamic compression (Kolsky bar, strain rates in the range of $\sim 10^3$ s⁻¹). A high-speed camera was used to observe the deformation and failure process of the specimen under dynamic loading. Cracking was observed along the loading axis under quasi-static compression. Under dynamic loading, nano-structured V fails in a very similar manner to nano-structured Fe and metallic glasses, i.e., via shear banding.

© 2003 Acta Materialia Inc. Published by Elsevier Ltd. All rights reserved.

Keywords: Nano-structured metals; bcc structure; Vanadium; Kolsky bar; Shear banding

1. Introduction

The plastic deformation mechanisms of nano-structured (NS) and ultrafine-grained (UFG) materials have drawn tremendous interest due to the scientific and technological importance of the problem. However, most of the documented experimental and theoretical work has been focused on metals with face centered cubic (fcc) crystalline structures [1–5]. For example, deformation twinning in nano-crystalline aluminum has been predicted via simulation [2,3], and recently observed using transmission electron microscopy [6]. Considering that deformation twinning is absent in conventional large-grained Al, this observation demonstrates a striking difference between the plastic deformation mechanisms of a conventional material and its NS counterpart. As for body centered cubic (bcc) metals such as iron, localized deformation in the form of shear bands has been reported for consolidated NS Fe under both dynamic and quasi-static compressive loading [7–

9]. Transmission electron microscopy (TEM) reveals that inside the shear bands, grains have been substantially elongated, suggesting that the shear banding process per se involves dislocation activities, and is of non-adiabatic nature. It is of interest to examine if these properties are unique to nano-structured Fe, or common for all nano-structured bcc metals [10–13]. A recent experiment suggests the latter, as shear banding was also observed in ultrafine-grained tantalum, [11]. In that case, however, the shear banding occurs at high strain rates and may be adiabatic.

In this work, we examine the behavior of nano-structured vanadium, another bcc metal. We have processed nano-structured V, with a moderately high melting temperature (1910 °C), by high-energy ball milling followed by two-step consolidation. The temperature of the final hot-consolidation was controlled to limit grain growth. We have characterized the microstructure of the consolidated, fully dense material using X-ray diffraction (XRD) and TEM. Mechanical properties of the nano-structured V were studied under both quasi-static (strain rates in the range of 10^{-3} – 10^0 s⁻¹) and dynamic (Kolsky bar, strain rates in the range of $\sim 10^3$ s⁻¹) compression. To observe the deformation and

* Corresponding author. Tel.: +1-410-516-5162; fax: +1-410-516-4316.

E-mail address: qwei@pegasus.me.jhu.edu (Q. Wei).

failure process, the side faces of the samples were polished to a mirror finish, and a high-speed camera was used to record a movie of the specimen under dynamic loading.

2. Experimental details

Vanadium powders (20 mesh) with a purity level of 99.5% were supplied by Alfa Aesar as the starting material for mechanical attrition and subsequent consolidation. Mechanical attrition was conducted using a SPEX 8000 high-energy mill with a vial and balls made of stainless steel (SS440). The weight ratio of balls/powder was 4:1. The balls and the vial were cleaned in an ultrasonic bath followed by drying in flowing air. The balls and vanadium granules were sealed into the vial in a pre-purged glove box in flowing Ar atmosphere to alleviate contamination. During milling, the system was constantly cooled using a fan. Typical milling time was 15 h. The internal grain sizes after milling was on the order of ~ 20 nm as revealed by XRD peak broadening.

A two-step consolidation procedure was used to obtain fully dense, NS vanadium. First, the milled powder was transferred into a WC die set in a flowing Ar atmosphere in order to reduce contamination. The powder was compacted at a pressure of ~ 1.0 GPa at room temperature for about 24 h, resulting in a green density of around 73% of the theoretical density. In the second step, the preform was transferred into another WC die set with a larger inner diameter for hot consolidation. This design of die set has the advantage of enhancing the densification process due to the existence of a shearing stress under compression which helps the removal of porosity [14]. Hot consolidation was performed with an HP20-4560-20 Hot Press (Thermal Technologies, CA). Several temperatures were used in search of the optimal condition under which fully dense material could be processed without loss of NS grain size. A pressure of 850 MPa was applied during hot consolidation for 3 h. It was found that the lowest consolidation temperature that can produce fully dense NS vanadium was 600 °C.

The densities of the consolidated specimens were determined by the buoyancy method based on Archimedes' principle. Vickers hardness was measured using a microhardness tester (Leco M-400). TEM was used for the microstructural analysis, especially the grain size, of the consolidated samples. TEM specimens were made by mechanical thinning to ~ 60 μm , followed by dimpling. Electron transparency was then obtained by ion milling. TEM was performed on a Philips EM-420 microscope operated at 120 KeV.

Quasi-static and dynamic compression samples were cut using electrical discharge machining. Dimensions of quasi-static samples are $3.0 \times 2.0 \times 2.0$ mm; those of dynamics samples are $2.5 \times 2.5 \times 1.6$ mm. Before loading,

the side faces were polished to a mirror finish for post loading microscopic observation. Quasi-static (strain rates in the range of 10^{-3} – 10^0 s^{-1}) compression tests were conducted using an MTS servohydraulic system. Dynamic compressive loading with strain rates of around 10^3 s^{-1} was performed using the Kolsky bar (or split Hopkinson bar) technique where the specimen is sandwiched between two elastic bars (called the input and output bars). Strain gages are cemented on the elastic bars to measure (i) the incident pulse generated by an impacting projectile, (ii) the reflected pulse from the input bar/specimen interface and (iii) the pulse transmitted through the specimen to the output bar. Kolsky bar techniques yield the highest possible strain rates in a uniaxial compression test under uniform deformation conditions. Details of the Kolsky bar technique can be found in [15]. A DRS Hadland Ultra 8 high-speed digital camera was used to record the deformation and failure process of the specimen under dynamic loading, using a framing rate of 200 kilo frames per second.

3. Results and discussion

Fig. 1 is the XRD pattern of the as-milled powder. Examination of all the peaks suggests significant peak broadening in comparison with the coarse-grained counterpart (also given in the figure). The full width at half maximum of the $\{110\}$ reflections is used to estimate the grain size inside the powder particles utilizing the Warren–Averbach [16] equation. The as-milled powders have a grain size of about 20 nm.

The Vickers hardness of a fully dense vanadium sample consolidated at 600 °C was measured to be ~ 6.0 GPa. The reported Hall–Petch relation for vanadium is [17]

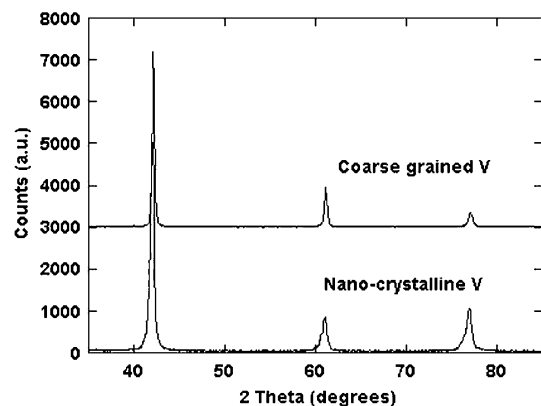


Fig. 1. XRD of the as-milled vanadium powder. Significant peak broadening can be observed for all the reflections. The full-width-half-maximum of $\{110\}$ reflections is used to estimate the internal grain size of the as-milled powder. For comparison, the XRD pattern of the annealed, coarse-grained V is also given in the figure.

$$\text{VHN} = 96.0 + 5.0d^{-1/2} \quad (1)$$

where d is the grain size in mm. Therefore, the Vickers hardness number of this sample corresponds to a grain size of ~ 100 nm. Fig. 2 displays the bright field TEM micrograph (A), the corresponding selected area diffraction (SAD) pattern (B), and a dark field TEM micrograph (C) taken from this sample. Analysis on the average grain size from TEM observations gives a value of about 100 nm, consistent with the Hall–Petch relation.

The quasi-static and dynamic compression stress–strain curves of annealed, coarse-grained vanadium are shown in Fig. 3 [18] for comparison with the behavior of nano-structured V. Annealed vanadium exhibits strain hardening under both quasi-static and dynamic loading, and the flow stress of annealed vanadium is a strong function of strain rate (the yield strength increases by a factor of more than 2 when the strain rate changes from

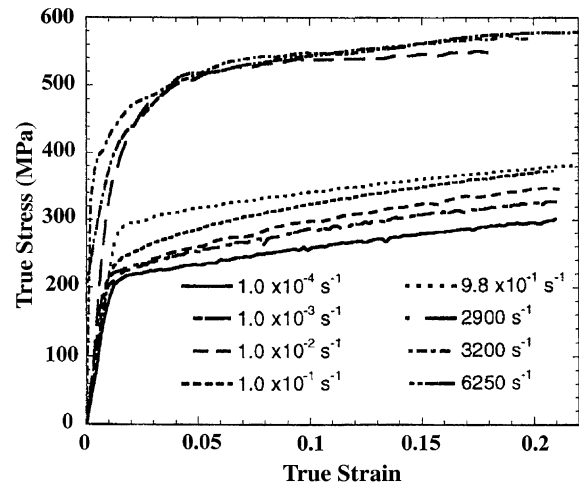


Fig. 3. Quasi-static and dynamic stress–strain curves for annealed vanadium under various strain rates. Note the strain hardening under both quasi-static and dynamic loading, and the rate dependence of the flow stress [18].

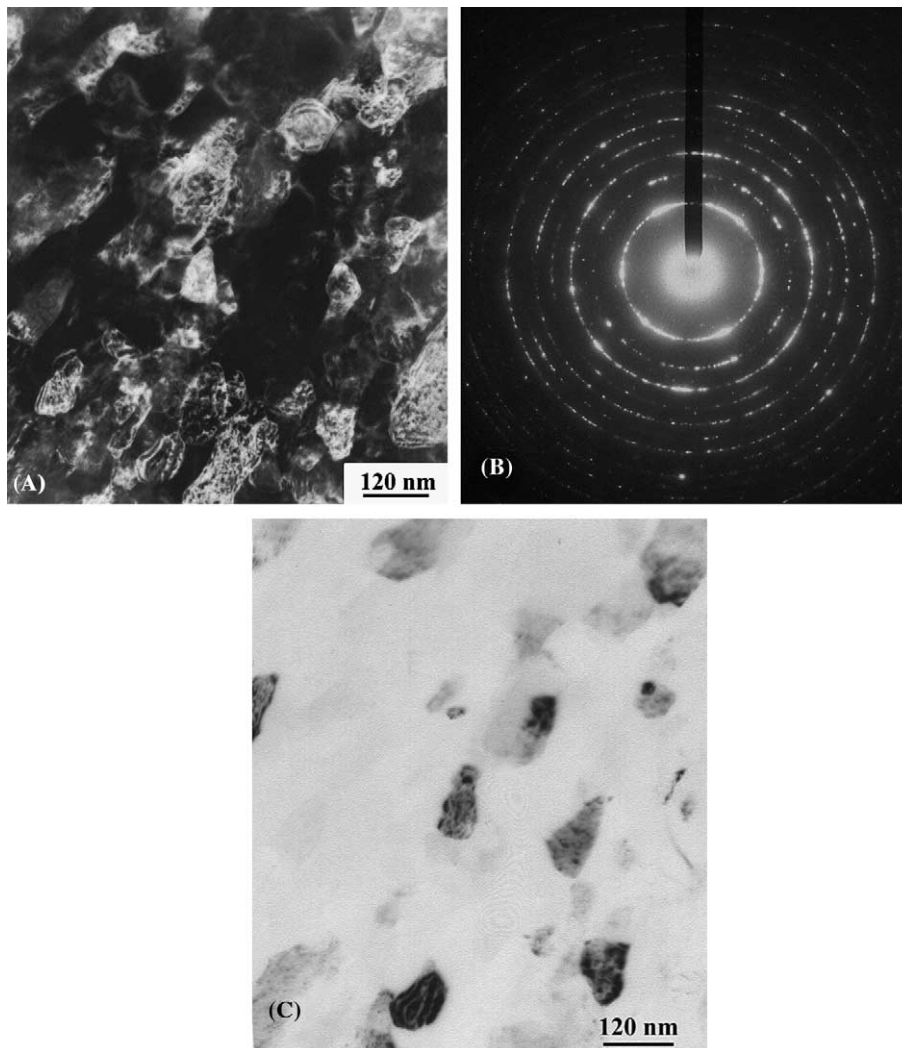


Fig. 2. Bright field TEM micrograph (A), SAD pattern (B) showing continuous rings corresponding to vanadium, and central dark field TEM micrograph (C) from the consolidated vanadium. The average grain size of the consolidated vanadium can be estimated to be around 100 nm.

the quasi-static to dynamic range), whereas the strain-hardening rate shows little dependence on the strain rate. If a power law ($\sigma/\sigma_0 = (\dot{\epsilon}/\dot{\epsilon}_0)^m$) is used to fit the experimental results at different strain rates, the value of the strain rate exponent m can be used as an indicator of the rate dependence of the material. In this work, the flow stresses of all the samples at an off-set strain of 0.10 are normalized against the flow stress (at the same 0.10 strain) of the sample loaded at a strain-rate of 10^{-2} s^{-1} . The m value of the annealed vanadium is computed to be ~ 0.05 , typical of annealed bcc metals.

Fig. 4 represents the stress–strain curves of the consolidated NS vanadium under compression at different strain rates. Under quasi-static loading, the yield strength is about 2 GPa, which is one third of the Vickers hardness value, in accordance with the empirical rule that for many materials the Vickers hardness number of a metal is three times of its yield strength. Some samples failed under quasi-static loading at a strain level of 0.05. Post-loading examination of the specimens shows microcracks along the loading axis. Fig. 5 displays one example of these cracks. However, catastrophic failure such as those of completely brittle materials was not observed in the NS vanadium in this study.

The quasi-static behavior of NS vanadium is different from that of consolidated NS Fe. For the latter, non-uniform deformation in the form of shear banding starts at a very early stage of plastic deformation [7–9]. This may be attributable to the stronger impurity sensitivity of vanadium than iron [19], which makes the consolidated NS vanadium less ductile than consolidated NS iron. Another possible reason is that the homologous temperature of the tests for NS V is only 0.14, which is lower than that of NS Fe (0.17). As a result, shear banding could be suppressed by the early initiation and propagation of cracks.

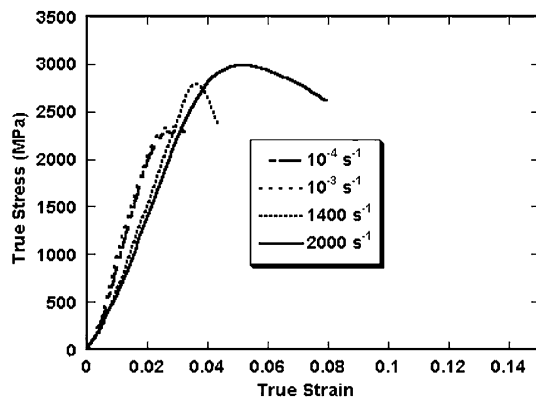


Fig. 4. Quasi-static and dynamic stress–strain curves at different strain rates for consolidated nano-structured vanadium with a grain size of approximately 100 nm. Note the substantially increased strength under both quasi-static and dynamic loading, and apparently reduced rate dependence of the yield strength as compared to the annealed state.

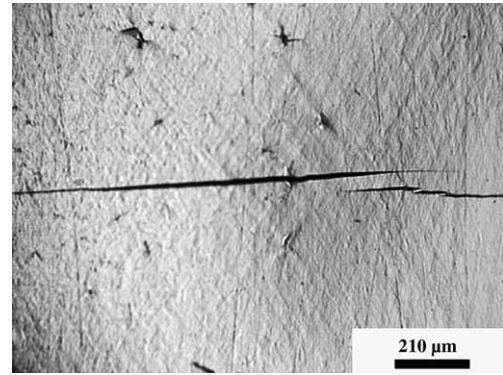


Fig. 5. Optical micrograph of the side face of a specimen after quasi-static compression. The compression loading is horizontal. Cracks parallel to the loading axis are apparent.

Fig. 4 also shows that under dynamic loading, the yield strength of NS vanadium is close to 3.0 GPa, almost 7 times higher than the dynamic yield strength of the annealed V. However, the effective strain rate hardening is decreased as compared to the annealed state (Fig. 3), consistent with the results for consolidated UFG and NS Fe [7–9], and with the model presented in [8] for bcc metals. An apparent load drop can be observed in every dynamic stress–strain curve. Fig. 6 shows three frames from the high-speed camera movie captured during the dynamic loading process. These snapshots may be used to explain the load drop during dynamic loading. Fig. 6(A) is the undeformed, or the original, state just before the loading pulse arrives. In Fig. 6(B), taken 5 μs later, initiation of a localized deformation zone can be observed at an angle of 45° with respect to the loading direction. This image corresponds to a true (overall) strain of 0.044. Due to the limited spatial resolution of the high-speed camera, it is likely that the localized deformation begins somewhat before this image was taken. In Fig. 6(C), the sample failed into three pieces when the true (overall) strain reached ~ 0.049 . We envisage that it is the localized deformation which eventually develops into cracks that leads to the load drop in the dynamic stress–strain curves. Therefore, under dynamic loading, shear banding prevails over crack initiation and propagation, and is the dominant deformation and failure mechanism. It is interesting to note that the dynamic failure mode of the NS vanadium sample is similar to consolidated NS Fe [7–9], both similar to the failure mode of bulk metallic glasses [20].

Assuming power law strain rate hardening as we did previously for annealed V, we can estimate the strain rate dependence of NS V, and the result is 0.014. This value of m is substantially smaller than that of the annealed, large grain V. Our experimental results on the mechanical behavior of bcc metals such as Fe and Ta have revealed reduction of rate dependence of the flow

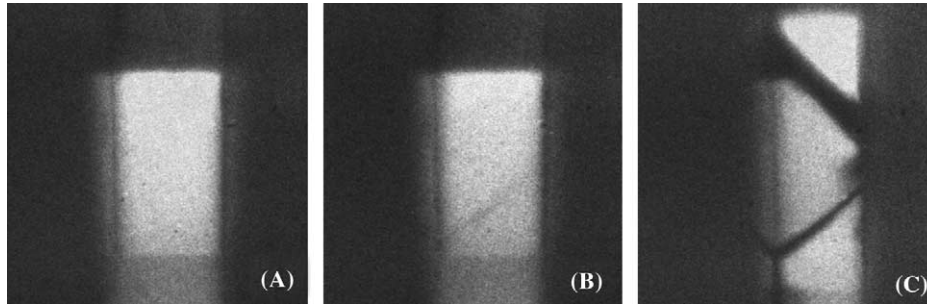


Fig. 6. High-speed camera snap-shots at different times during the dynamic loading process of NS vanadium. Loading is horizontal. The strain rate of the test is 2000 s^{-1} . The three images correspond to an apparent strain of 0.0, 0.044 and 0.049. (A) is the undeformed state. Initiation of shear localization can be observed in (B), which corresponds to a strain level of 0.044, and (C) shows the shearing failure of the specimen, at a nominal strain of 0.049.

stress upon refining the grain size of the material into the UFG and NS regime. As seen here again for V, it appears that UFG or NS bcc metals exhibit substantially decreased work hardening (or apparent softening). The combined effects of decreased work hardening and reduced strain rate hardening, and the substantial grain size strengthening explain, at least in part, the enhanced tendency for shear localization in the consolidated NS vanadium [21,22].

4. Summary and concluding remarks

1. Fully dense, nano-structured vanadium has been successfully produced using ball milling and a two-step consolidation method.
2. The Vickers hardness of the NS vanadium consolidated at $600 \text{ }^\circ\text{C}$ was 6.0 GPa, suggesting a nano-crystalline grain size of 100 nm according to the known Hall–Petch relation for vanadium. This grain size was confirmed in TEM observations.
3. Under quasi-static compression, the yield strength of the NS vanadium (d of 100 nm) was measured to be 2.0 GPa. Cracking occurred early during plastic deformation along the loading axis, suggesting that the NS vanadium is rather brittle, possibly due to impurity effects.
4. Under dynamic loading, nano-structured V fails in a manner similar to the failure of consolidated NS Fe and bulk metallic glasses, i.e., via shear banding.
5. Compared to the annealed vanadium with large grain sizes, the NS vanadium would exhibit reduced strain hardening and strain rate dependence, both of which are factors promoting the shear localization observed.
6. The similarities observed between V and Fe [7–9] corroborate that nano-crystalline and ultrafine grain sizes have strong effects on the deformation/failure properties. These effects appear to be common for metals with the bcc structure.

Acknowledgements

This work was performed under the auspices of the Center for Advanced Metallic and Ceramic Systems (CAMCS) at the Johns Hopkins University. This research was sponsored by the Army Research Laboratory (ARMAC-RTP) and was accomplished under the ARMAC-RTP Cooperative Agreement no. DAAD19-01-2-0003. The views and conclusions contained in this document are those of the authors and should not be interpreted as representing the official policies, either expressed or implied, of the Army Research Laboratory or the US Government. The US Government is authorized to reproduce and distribute reprints for Government purposes not withstanding any copyright notation hereon.

References

- [1] Weertman JR, Farkas D, et al. *MRS Bull* 1999;24:44.
- [2] Yamakov Y, Wolf D, Phillpot SR, Mukherjee AK, Gleiter H. *Nature Mater* 2000;1:45.
- [3] Yamakov Y, Wolf D, Phillpot SR, Gleiter H. *Acta Mater* 2002;50:5005.
- [4] Hasnaoui A, Van Swygenhoven H, Derlet PM. *Science* 2003;300:1550.
- [5] Wang Y, Chen M, Zhou F, Ma E. *Nature* 2002;419:912.
- [6] Chen M, Ma E, Hemker K, Sheng H, Wang Y, Cheng X. *Science* 2003;300:1275.
- [7] Wei Q, Jia D, Ma E, Ramesh KT. *Appl Phys Lett* 2002;81:1240.
- [8] Jia D, Ramesh KT, Ma E. *Acta Mater* 2003;51:3495.
- [9] Jia D, Ramesh KT, Ma E. *Scripta Mater* 2000;42:73.
- [10] Wei Q, Kecskes L, Jiao T, Hartwig KT, Ramesh KT, Ma E. Adiabatic shear banding in ultrafine-grained Fe processed by severe plastic deformation. *Acta Mater* (to be submitted).
- [11] Wei Q, Jiao T, Mathaudhu SN, Ma E, Hartwig KT, Ramesh KT. *Mater Sci Eng A* 2003;358:266.
- [12] Wei Q, Jiao T, Ramesh KT, Ma E. Shear localization in pure tungsten. *Appl Phys Lett* (to be submitted).
- [13] Jia D. PhD Thesis of The Johns Hopkins University, 2001.
- [14] German RM. *Sintering theory and practice*. John Wiley & Sons Inc.; 1996.
- [15] Follansbee PS. The Hopkinson bar. In: Davis JR, Refnes SK, editors. *Metals handbook* 9th ed, vol. 8. Ohio: ASM Metals Park; 1985. p. 198–203.

- [16] Warren BE. X-ray diffraction. Dover Publications Inc.; 1990.
- [17] Nouet G, Deschanvres A. *J Less Com Metals* 1974;35:17.
- [18] Lennon A. PhD Thesis of The Johns Hopkins University, 1998.
- [19] Conrad H. In: Zackey VF, editor. High-strength materials. John Wiley & Sons, Inc.; 1965.
- [20] Hufnagel TC, Jiao T, Li Y, Xing LQ, Ramesh KT. *J Mater Res* 2002;17:1441.
- [21] Bai Y, Dodd B. Adiabatic shear localization. Pergamon Press; 1992.
- [22] Wright TW. The physics and mathematics of adiabatic shear bands. Cambridge University Press; 2002.